Comprehensive pilot-scale investigation of seawater nanofiltration softening by increasing permeate recovery with recirculation

Yuefei Song[a], Tiemei Li[a], Jianguo Zhou[a,*], Feng Pan[a], Baowei Su[b,c], Congjie Gao[b,c]

[a]Key Laboratory of Yellow River and Huai River Water Environmental and Pollution Control, Ministry of Education, School of Environment, Henan Normal University, 46 East of Construction Road, Xinxiang 453007, China, emails: songyuefei@htu.cn (Y. Song), tiemeili@126.com (T. Li), jianguozhou1962@163.com (J. Zhou), fengpan@htu.cn (F. Pan)
[b]Key Laboratory of Marine Chemistry Theory and Technology, Ministry of Education, Ocean University of China, 238 Songling Road, Qingdao 266100, China, emails: subaowei@ouc.edu.cn (B. Su), gaocjie@mail.hz.zj.cn (C. Gao)
[c]College of Chemistry & Chemical Engineering, Ocean University of China, 238 Songling Road, Qingdao 266100, China

Received 28 November 2014; Accepted 13 August 2015

ABSTRACT

Two commercial nanofiltration (NF) modules and one tight ultrafiltration module (with molecular weight cut-off of 20 kDa) were assembled to two integrated membrane systems to investigate comprehensively the NF efficiency of seawater softening. The effect of increasing NF permeate recovery (R_{NF}) by recirculation and dosage of chemicals on the observed and the real NF separation performance, concentration polarization extent was evaluated. The results showed that under both HCl acid and antiscalant dosage condition (termed as Scheme II), the superior softening performances with 87.7–93.5% of the observed and 88.5–93.9% of the real total hardness removals were achieved at constant inlet cross-flow velocity of 0.05 m s^{-1}, pressure of 2.02–2.67 MPa, temperature of 21–22°C, and NF retentate recycle ratio (R_r) of 1.69–37.16. The Ca^{2+}, Mg^{2+}, and SO$_4^{2-}$ ionic concentrations and the total hardness value in NF permeate with R_{NF} at 65%, and NF permeate flux at 6.24 L m^{-2} h^{-1} in Scheme II were only around 176, 84, 45, and 798 mg L^{-1}, which was much lower than that in typical SWRO feed streams, and indicated that NF90-4040 (termed as NF1) membrane under chemicals dosage yielded a relatively high efficiency of seawater softening.

Keywords: Nanofiltration; Integrated membrane system; Seawater softening; High NF permeate recovery; Concentration polarization

1. Introduction

Water softening, which refers to the removal of hardness due to the presence of certain ions including calcium, magnesium, and other metal cations (e.g. iron(II) and manganese(II)) from water, can help to alleviate problems caused by hard water, such as hindering of laundering processes and scale buildup in hot water pipes and heater [1,2]. Conventionally, hardness can be removed by ion exchange resins containing sodium/potassium, which can be displaced by calcium/magnesium. The disadvantage of this process is that total dissolved salts increase as a whole in the water as the ion exchanger releases two sodium ions for every one calcium or magnesium ion captured. It also consumes the salt brine that is used for regeneration, which is unbeneficial

*Corresponding author.

to treat seawater, brackish water, and other hardness-enriched water [2,3].

In contrast, membranes offer a possible way to solve the above-mentioned problems. Nanofiltration (NF) is a relatively new membrane technology and more recently development in the filtration field. NF membrane is typical with molecular weight cut-off (MWCO) of 300–1,000 Da and lower operating pressure of 0.4–3.0 MPa [4–8]. In regards to both the size of separated species and pressure involved, NF has an intermediate position between ultrafiltration (UF) and reverse osmosis (RO). In addition, NF membranes in contact with solution are also charged due to the dissociation of surface functional groups or adsorption of charge solute, which affect membrane separation performance for inorganic salts [9,10]. Both the molecular sieving mechanism and electrostatic effects are the major factors which affect the transport of charged solutes through the membrane [9,11]. As a consequence, NF has a unique separating characteristic of preferentially rejecting divalent or multivalent ions which are the main sources to cause hardness mineral deposition in seawater desalination. For this reason, NF separating process has been recognized as a key technology to be suitable for seawater softening prior to desalination processes by RO, multistage flash, and multiple effect distillation, oilfields water injection and oily waste reusing processes.

In the past few years, great efforts have been made in improving the NF performance and the efficiency of seawater softening. Drioli et al. [12] investigated the utilization of NF for the removal of hardness and most multivalent ions, and concluded that the recovery factor of a coupled NF−RO seawater desalination system was 10–12% higher than that of a SWRO plant based on conventional pretreatment. Su et al. [13] studied on seawater NF softening technology for offshore oilfield polymer solution preparation and found that with the properly selected NF membrane, which could keep more than 90% removal rate for Ca^{2+} and Mg^{2+}. Bader [14] adopted NF module to provide nearly sulfate-free seawater to oil fields in treating seawater from the North Sea. Nanda et al. [2] evaluated the performance of ESNA1 and EDA NF membranes for seawater softening at various feed pH values. However, these above-mentioned studies were partly related to high NF permeate recovery (R_{NF}) in two or three stages. When didn't take the amplification effect into account in those processes, the R_{NF} for single element were all lower than 50%.

Recovery is one of the key design parameters which determines the scale and cost of a seawater membrane separation system [15]. Higher water recovery will result in smaller installation size of the sep-

aration system and less capital and operating costs. Therefore, efforts must be taken to increase R_{NF} in seawater NF softening process. The process during R_{NF} increasing always associates some operating parameters or softening performance variation in different degrees. Hasson et al. [16] conducted NF experiments for seawater softening, and found that under same operating conditions of applied pressure of 3.1 MPa, the permeate recovery at the reduced feed flow rate of 20.2 L h^{-1} was 46% compared to only 30% when the feed flow rate was increased to 34.6 L h^{-1}. Su et al. [17] applied NF400-8040 membrane in the dual-stage NF system to soften seawater, and found that the decrease in R_{NF} for the first stage from 47.2 to 39.2% and for the second stage from 23.8 to 15.1% accompanied by an increase in the influent flow rate from 5,300 to 8,700 L h^{-1}.

However, one of the critical factors in applying seawater NF softening process must be taken into account is the concentration polarization (CP) effect [18]. Because CP increases the transmembrane osmotic pressure, which results in the decrease in driving pressure, as well as permeate flux, and hence causes the degradation of softening performance. Previously, reports showed that there was a significant difference between measurement and calculation for the more highly concentrated electrolyte solution [19,20]. Freger et al. [19] compared the observed flux and the calculated flux based on a correction model, to show that for a salt concentration lower than 4% (w/v), predictions agreed with the measured values, but for more concentrated solutions (>9% (w/v)), the observed flux was 1.3 times larger than the predicted flux. Capelle et al. [20] also found that for a high salt concentration (10% (w/v)), experimental results could no longer be explained in terms of osmotic pressure correction. Nevertheless, rare research focused on the CP effect on seawater NF softening performance.

In this study, the treatment alternatives were covered by two integrated membrane systems (IMSs) with two commercial NF modules and one tight UF module (with MWCO of 20 kDa). The comprehensive pilot-scale performance of seawater softening was evaluated under chemicals addition conditions at Yellow Sea of China. Therefore, NF membrane seawater softening performance was evaluated by combing R_{NF} factor and CP effect in the alternative pilot-scale UF−NF trains. The results obtained in this study are expected to build deeply and completely understanding of NF seawater softening effect, and find the optimum operating conditions that are specific to the given membranes, feed water, and as high as possible of R_{NF} value.

2. Material and methods

2.1. membranes

One tight commercial hollow fiber UF membrane module of polysulfone (PS) was used and the MWCO of which was 20 kDa. NF experiments were performed using two tight types of commercial spiral-wound membrane modules named NF90-4040 (termed as NF1) and BDX-N90-4040 (termed as NF2), supplied by Dow Filmtec and Beidouxing membrane Co. Ltd, respectively. Based on the manufactures' data sheet and literature [21,22], the characteristics of the membrane modules are summarized in Table 1.

Hydrochloric acid (analytical reagent) and one commercial antiscalant, Polyamino Polyether Methylene Phosphonate (PAPEMP) from Shandong Taihe Water Technologies Co. Ltd, China, were used to illustrate the present approach of evaluating and comparing chemicals dosage effectiveness in NF softening processes.

2.2. Experimental setup and procedure

An appropriate seawater pretreatment approach should provide feed water with low value of turbidity and Silt Density Index (SDI) continuously and stably for NF membrane. Compared with conventional pretreatment process, UF technology has many advantages, such as consistent and high quality of filtrate independent of raw seawater quality, simplicity of operation, and maintenance [23]. Therefore, UF was selected as the pretreatment technology of NF, and the NF performance of seawater softening by increasing R_{NF} in UF–NF IMS was investigated comprehensively. The flow diagram of the IMS with a capacity of
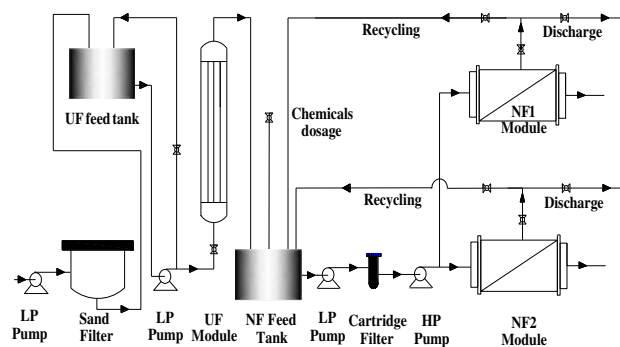
Fig. 1. Flow diagram of the integrated UF–NF system for seawater softening.

3–5 m^3 d^{-1} is depicted in Fig. 1. The pilot study was conducted at Qingdao Jiaozhou Bay, the Yellow Sea of China.

Raw seawater was firstly pumped through cartridge sand filter to the UF module, the UF filtrate was further pumped to NF module to obtain NF softening product water. All water sources, such as UF concentrate and backwashing water as well as partially NF retentate, were collected and drained to the sea via the injection tank on site.

Before each sampling, at least 2 L solution was discharged to assure sampling accuracy. The data including operating pressure and flow rate in feed water, retentate and permeate for UF and NF membranes per 20 min were recorded. After each run, NF membrane was flushed three times using deionized water for 20 min at pressure of 0.65 MPa and cross-flow velocity of 0.068 m s^{-1} to recover membrane flux.

Table 1
Material characteristics and module details of the membrane system

Items	UF	NF1	NF2
Manufactory	Lanlu	Filmtec	Bluestar
Module type	HF-1500	NF90, 4040	BDX4040N-90
Module configuration	Hollow fiber	Spiral wound	Spiral wound
Membrane materials	PS	Polyamide	Polyamide
MWCO (kDa)	20	0.1	0.1–0.5
Membrane effective area (m^2)	8	7.6	7.5
Pure water flux (L m^{-2} h^{-1} MPa^{-1})	2,419.3	28.8	20.4
Pore size (nm)	10	0.99	1–2
Salt rejection (%)	≈0	>85%[a]	>85%[b]
Range of feed temperature (°)	0–50	0–45	0–45
Range of feed pH	2–11	3–10	2–11
Range of pressure (MPa)	0–0.2	0–4.1	0–4.1

Note: The values were obtained under following conditions:
[a]NF operating pressure 1.0 MPa, feed temperature 25℃, 500 mg L^{-1} NaCl solution, the recovery rate 15%.
[b]NF operating pressure 1.55 MPa, feed temperature 25℃, 2000 mg L^{-1} NaCl solution, the recovery rate 15%.

Table 2
Four different operating conditions

Parameters	Scheme I	Scheme II	Scheme III	Scheme IV
Train	UF−NF1	UF−NF1	UF−NF2	UF−NF2
Feed pH	7.8 ± 0.03	5.0	7.8 ± 0.03	5.0
Addition of acid	No	HCl	No	HCl
Concentration of antiscalant (mg L^{-1})	0	10	0	10
Addition of antiscalant	No	PAPEMP	No	PAPEMP

A semi-closed loop mode NF experiments were carried out at constant inlet cross-flow velocity of 0.05 m s^{-1}. Desired R_{NF} could be achieved mainly by regulating the flow rates of the discharge and the recycling stream of the retentate, respectively. The other auxiliary measure also adopted in the initial phase is increasing operating pressure to assist to fulfill the objective R_{NF}. A series of R_{NF} including 10, 15, 20, 25, 30, 35, 40, 45, 50, 55, 60, and 65% were chosen, respectively.

Table 2 clarifies the specific operating conditions in four different schemes for the NF membrane module. The pH of the feed was adjusted to 5.0 with HCl acid, and the concentration of the antiscalant in the feed was kept constantly at 10-mg L^{-1} under antiscalant addition condition. This relatively high concentration was chosen in order to reliably and safely increase the R_{NF} as much as possible.

2.3. Analysis methods

Samples were collected in polyethylene bottles, tightly capped and stored at 4℃ until analysis. Concentration of the main inorganic ions (K$^+$, Na$^+$, Ca^{2+}, Mg^{2+}, Cl$^-$, and SO$_4^{2-}$) were measured with a Dionex ICS-3,000 Ion Chromatography (Dionex, USA); TDS was calculated as the summation of the concentration of the main ions; turbidity was measured by turbid meter LP-2001 (Hanna, Italy); SDI of raw seawater and UF filtrate was measured by a SDI monitor (Millipore, America); conductivity was measured by conductivity meter Orion 145A+ (Thermo, America); pH was measured by precision acidity meter DELTA 320 (Mettler Toledo, China). Each sample was measured two times and if the values of the two measurements deviated only slightly, then the average value was used, otherwise, sample was detected more times to obtained accepted results. The relative standard deviation of the measurements was less than 2%.

2.4. Calculated parameters

2.4.1. Basic related parameters

To describe the overall operating conditions for the NF module, R_{NF}, NF retentate recycle ratio (R_r), and the permeate flux (J_v) were used, as defined in Eqs. (1)–(3), respectively [24]:

$$R_{NF} = \frac{Q_p}{Q_p + Q_{r1}} \qquad (1)$$

$$R_r = Q_{r2}/Q_{r1} \qquad (2)$$

$$J_v = Q_{r1}/A \qquad (3)$$

where Q is the flow rate; A is the effective membrane area; Subscripts p, $r1$, and $r2$ refer to the permeate, retentate, and recycle streams of the NF module.

2.4.2. Concentration polarization and real rejection parameters

Concentration polarization increases transmembrane osmotic pressure, which results in decrease of effective pressure difference, as well as permeate flux, and hence causes the degradation of separating performance. The extent of concentration polarization, termed as the CP modulus, is the ratio of the solute concentration at the membrane surface to that in the bulk brine. CP is determined using Eqs. (4)–(6) [25,26]:

$$CP = \frac{c_m}{c_b} \qquad (4)$$

$$\frac{c_{m,i} - c_{p,i}}{c_{b,i} - c_{p,i}} = e^{\frac{J_v}{k_i}} \qquad (5)$$

$$k_i = 0.5510 \left(\frac{u d_h}{v}\right)^{0.4} \left(\frac{v}{D_i}\right)^{0.17} \left(\frac{c_{b,i}}{\rho}\right)^{-0.77} \left(\frac{D_i}{d_h}\right) \qquad (6)$$

where CP_i is the CP modulus of solute i; $c_{m,i}$, $c_{b,i}$, $c_{p,i}$ are the concentrations of the rejected solute i at the membrane surface, in the bulk brine, and in the permeate stream, respectively; J_v is the permeate flux; k_i is the solute mass transfer coefficient; d_h is the hydraulic diameter of the feed cross-flow channel; D_i is the solute diffusivity; u is the average cross-flow velocity of the feed channel; ρ and v are the average

density and kinematic viscosity of the retentate stream, respectively.

Due to the effect of CP, solute concentration at the surface of solute-rejecting membrane is higher than solute concentration in the bulk solution. The difference between the experimentally observed rejection (R_{obs}) and the real rejection (R_{real}) must be taken into account. And they are defined as the following equations [9,27]:

$$R_{obs} = 1 - \frac{c_{p,i}}{c_{f,i}} \tag{7}$$

$$R_{real} = 1 - \frac{c_{p,i}}{c_{m,i}} \tag{8}$$

where $c_{f,i}$ is the concentration of the rejected solute i in the feed water.

3. Results and discussion

3.1. Pilot test of UF pretreatment

The performance of the UF module with filtration of cross-flow mode remained stable because of backwash procedure during the testing period. The operating parameters for UF unit were optimized according to our prior work [11] and kept constant in this test, and the UF filtrate flux and product water recovery of seawater in this test were kept constantly at about 150 L $(h \, m^2)^{-1}$ and 95% under 0.09 MPa. All SDI_{15} values of UF filtrate were below 3.1 and turbidity values were relatively stable at about 0.01 NTU. It indicates that UF filtrate quality can meet the demand of NF feed despite the variation of the raw seawater quality. Table 3 summarizes the characteristics of the NF feed water quality parameters, such as SDI, turbidity, alkalinity, and hardness as well as the main ionic concentrations, which were measured in site.

3.2. Pilot test of seawater NF softening process

3.2.1. The operating parameters of the NF module

The main operating parameters include operating pressure, feed temperature, and NF retentate R_r.

The variation of operating pressure and feed temperature with R_{NF} during each scheme is presented in Fig. 2. On the whole, it could be seen that the operating pressure increased rapidly in the beginning and then quite slightly with R_{NF} when these two low selectivity NF membranes were adopted. For example, a large (30%) rise in NF operating pressure when R_{NF} was increased 10–20% in Scheme I was observed, but a small (3%) rise happened in the period of 20–65%. This can be explained that, as mentioned earlier, the contributing factor of increasing operating pressure occurs at first in the R_{NF} enlargement processes. But the goal of R_{NF} continues to increase gradually for NF modules (when R_{NF} larger than 20% for NF1 and 15% for NF2, respectively) can be achieved through a growing proportion of NF retentate recycled back to the feed water supply tank. Accordingly, it causes a slight increase in salt concentration and osmotic pressure of the feed water. So the operating pressure increases slightly with R_{NF}. It could also be seen from Fig. 2 that at the same R_{NF}, there was small discrepancy in operating pressure values among the four schemes. The operating pressure of Schemes II and IV are slightly higher, which might be due to the excessive addition of antiscalant and resulting as foulants to some extent [28]. At the same time, NF feed inlet temperature showed little change and ranged between 21 and 24°C because of the weather changes during the test period.

In the NF module, according to Eq. (2), different NF retentate R_rs would be needed to fulfill the varied R_{NF} test. With the increase in R_{NF} from 10 to 65%, more and more great proportion of the NF retentate would be recycled and mixed with the NF feed. The variation of R_r with R_{NF} at different schemes is shown in Fig. 3. It could be noticed that the increase in R_{NF}

Table 3
Main parameters of the NF feed water

Parameters	Values	Parameters	Values
Turbidity (NTU)	<0.1	K^+ (mg L^{-1})	363–405
SDI_{15}	<3.1	Na^+ (mg L^{-1})	9,260–11,451
TDS (mg L^{-1})	31,527–35,562	Ca^{2+} (mg L^{-1})	372–419
Total hardness (mg L^{-1})	3,190–3,480	Mg^{2+} (mg L^{-1})	1,150–1,325
Total alkalinity (mg L^{-1})	1.95–2.26	Cl^- (mg L^{-1})	17,500–19,565
COD_{Mn} (mg L^{-1})	1.4–2.0	SO_4^{2-} (mg L^{-1})	2,100–2,396
Activity of SiO_2 (mg L^{-1})	0.36–0.90	pH	7.8 ± 0.03

Note: The total hardness and total alkalinity according to $CaCO_3$ terms.
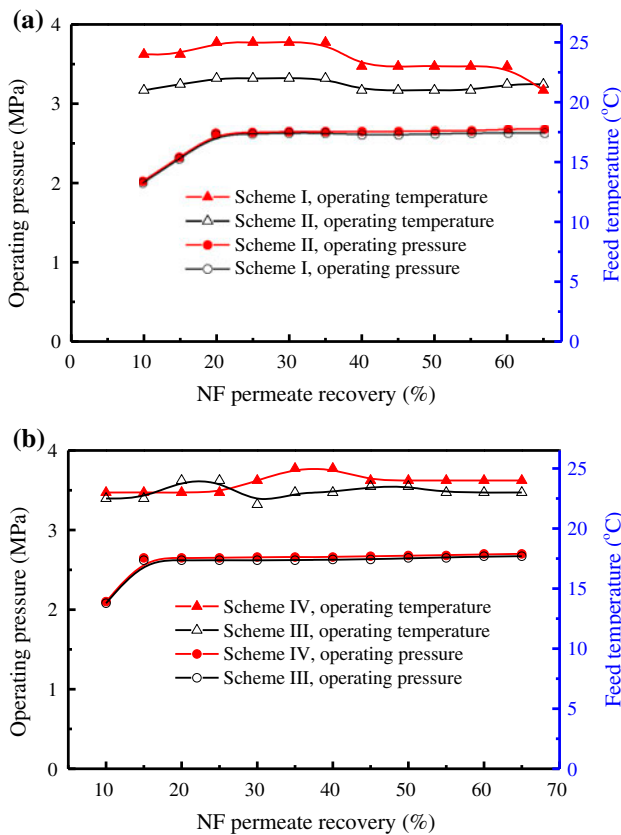
Fig. 2. The variation of operating pressure and feed water temperature with R_{NF} under inlet cross-flow velocity of 0.05 m s^{-1} ((a) NF1 and (b) NF2).
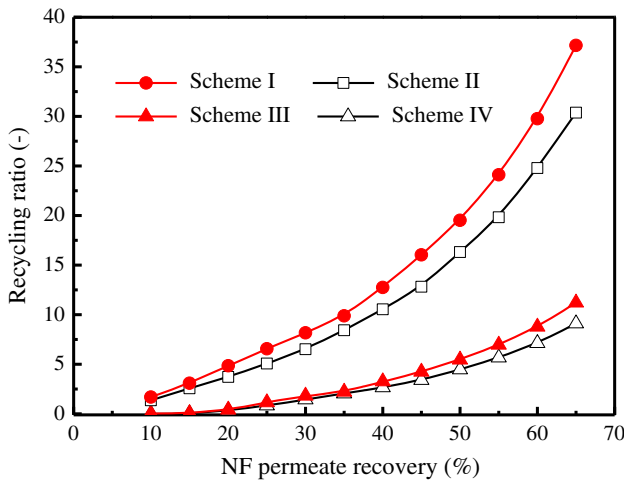
Fig. 3. Influence of R_{NF} on the recycling ratio under inlet cross-flow velocity of 0.05 m s^{-1}.

from 10 to 65% was accompanied by an increase in R_r from 1.69, 1.37, 0.04, and 0.01 to 37.16, 30.38, 11.21, and 9.11 in Schemes I–IV processes, respectively. For

Schemes II and IV, the acid and antiscalant dosage induced a significant descent of the R_r under the same R_{NF}, which implied that with chemicals addition, smaller R_r value can be attained for the same higher R_{NF}. Comparatively, for Schemes I and III, where neither acid nor antiscalant was dosed, under the same operating pressure, the NF permeate flow rate decreased, in order to keep the same R_{NF}, NF recycle stream flow rate should be increased. Therefore, higher R_r would be needed to achieve the same R_{NF}.

It could be also seen from Fig. 3 that under the same R_{NF}, R_r values in Schemes I and II were always much higher than those in Schemes III and IV. The higher average NF retentate R_r values were obtained in Schemes I and II processes with the increase ratio of 283 and 269% compared to those in Schemes III and IV processes, respectively. This phenomenon could be attributed to the larger difference between the permeate flux of NF1 and NF2. It can be concluded from Eqs. (1)–(2) that under the same R_{NF} and inlet cross-flow velocity of 0.05 m s^{-1} for NF module, R_r is inversely proportional to the NF permeate flow rate and the flux.

3.2.2. The variation of permeate flux

Trends of NF steady-state permeate flux as a function of R_{NF} in different schemes are shown in Fig. 4. In general, the entire NF permeate fluxes in the four schemes initially increased sharply and decreased gradually afterward with the ascending R_{NF}. For example, in Schemes III and IV processes as shown in Fig. 4, when R_{NF} was evaluated from 10 to 15%, the
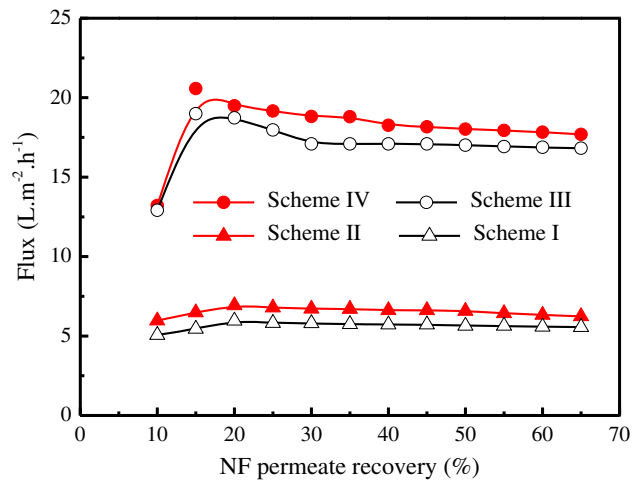
Fig. 4. Dependence of NF permeate flux on R_{NF} under inlet cross-flow velocity of 0.05 m s^{-1}.

permeate flux increased rapidly from 12.91, 13.21 to 18.99, 20.57 L m^{-2} h^{-1}, respectively. And then this value decreased gently to 16.82 and 17.69 L m^{-2} h^{-1} when R_{NF} was evaluated continuously to 65%.

The steady-state permeate fluxes of NF module in Schemes II and IV were a little higher than the corresponding values in Schemes I and III processes within the testing range of R_{NF}. The higher average NF permeate fluxes were obtained in Schemes II and IV processes with the increase ratio of 6.5 and 15.8% compared to those in Schemes I and III processes, respectively. This phenomenon could be attributed to the elimination of alkaline scale at low pH [29,30]. The permeate flux of the NF1 module in Schemes I and II processes were much smaller than the NF2 module in Schemes III and IV processes. This could be due to the relative larger difference in membrane properties existing for the candidate membranes, such as pore size and MWCO, which can be seen in Table 1.

3.2.3. The variation of the observed rejection of divalent ions

The main divalent ions observed rejection by NF membranes vs. R_{NF} is shown in Fig. 5. The salt rejections (calculated with conductivity and TDS, respectively) by NF membranes are also plotted in Fig. 5 for comparison with the membranes' selectivity of divalent ions over monovalent ions. It can be seen that the salt rejection and all the main divalent ions' observed rejection by NF membranes increased in the beginning and then decreased gradually in the testing R_{NF} range. For example, when R_{NF} increased from 10 to 65%, the rejection of Ca^{2+}, Mg^{2+}, SO$_4^{2-}$, conductivity, and TDS increased at first from 69.23, 95.04, 98.69, 64.87, and 66.78% to 70.62, 96.21, 98.97, 69.07, and 72.28%, and then decreased finally to 53.15, 92.62, 97.86, 44.17, and 45.89%, in Scheme I process, respectively. By contrast, at Scheme III, an ascending of R_{NF} from 10 to
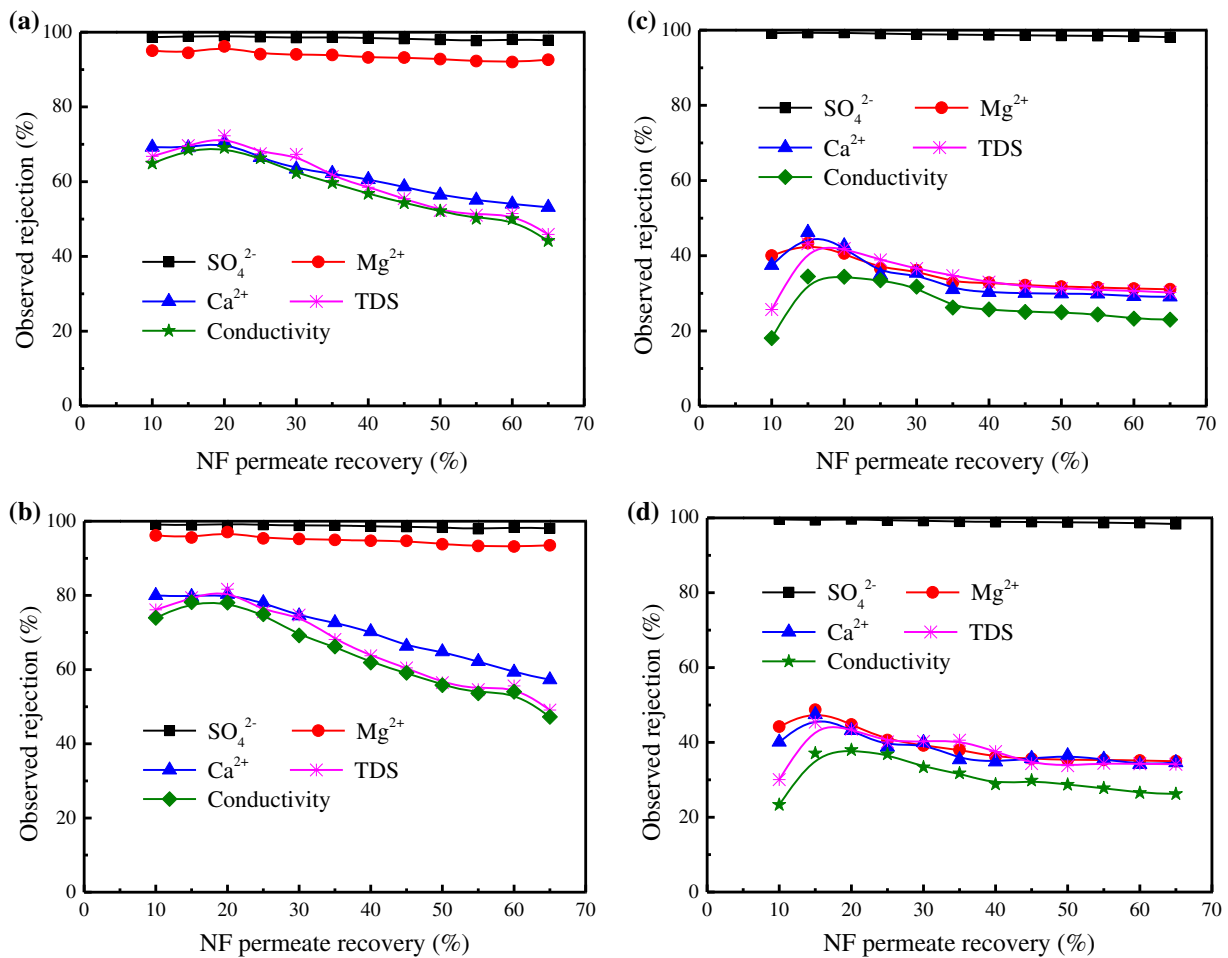
Fig. 5. Trends of the observed rejection as function of R_{NF} ((a) Scheme I, (b) Scheme II, (c) Scheme III, and (d) Scheme IV).

65% resulted in a rise of the rejection of Ca^{2+}, Mg^{2+}, SO_4^{2-}, conductivity and TDS at first from 37.47, 40.03, 99.22, 18.08, and 25.69% to 46.21, 43.37, 99.34, 34.47, and 43.2%, and then decreased finally to 29.06, 31.09, 98.17, 23.01, and 30.22%, respectively. The observed salt rejection and main divalent ions rejection in Schemes II and IV were relatively higher than those in Schemes I and III. This could be explained by the conversion of HCO_3^- into carbon dioxide, and the complex of Ca^{2+} and Mg^{2+} ions by antiscalant [31]. Therefore, less amount of divalent ions and HCO_3^- permeated the membrane, resulting in a relatively higher observed salt rejection and main divalent ions' rejections in Schemes II and IV.

It was also noticed that the numerical values between salt rejection and the main divalent ions rejection for these two candidate NF membranes are apparently different. The salt rejection values and the most divalent ions rejection by NF1 membrane were larger than 40%, especially for SO_4^{2-} ion rejection, which were always kept above 96%. This high divalent ions rejection by NF1 membrane offers a viable

and potential option for seawater softening. But the capacity of removing the main divalent ions by NF2 membrane is relatively poorer.

3.2.4. The variation of total hardness

Fig. 6 clearly showed that when R_{NF} increased from 10 to 65%, the removal efficiency of total hardness decreased after an initial increase with R_{NF}. In this experiment, it could be obviously found that under the same R_{NF}, NF1 process yields the higher total hardness rejection. For example, in NF1 process, the rejection of total hardness is 85.89 and 87.71% at the R_{NF} of 60% in Schemes I and II, while in NF2 process, this value is 30.92 and 34.98% in Schemes III and IV, respectively. Correspondingly, the values of total hardness in NF1 permeate are much lower than that
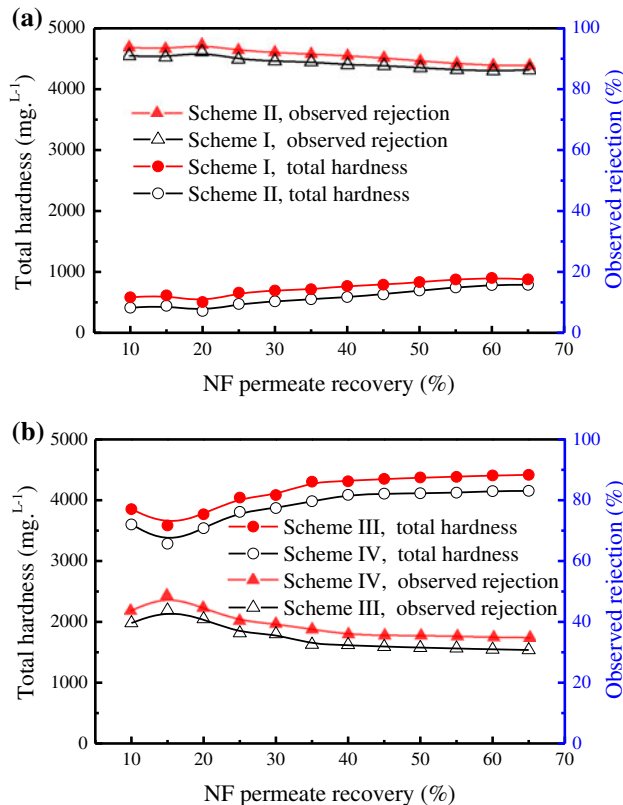
Fig. 6. Trends of total hardness in NF permeate, and the observed total hardness rejection as function of R_{NF} ((a) NF1 and (b) NF2).
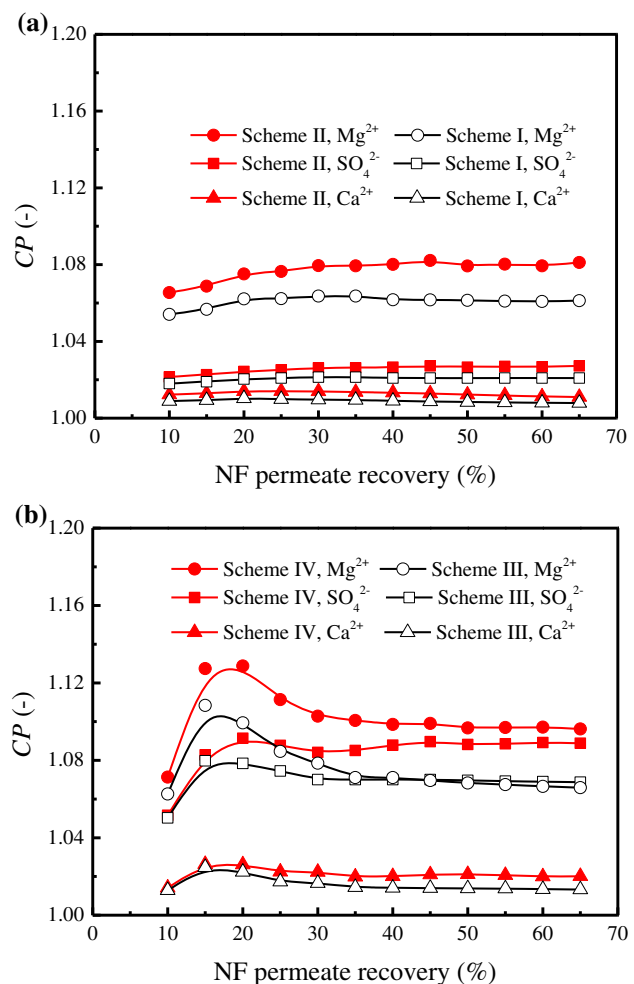
Fig. 7. Dependence of CP of Mg^{2+}, SO_4^{2-}, and Ca^{2+} ions on R_{NF} in the IMS ((a) NF1 and (b) NF2).

in NF2 permeate at the fixed R_{NF}. The values of total hardness in NF1 permeate are all less than 900-mg L^{-1}, but are all larger than 3,200-mg L^{-1} in NF2 permeate. It indicates that NF1 membrane yields a relatively high efficiency of seawater softening.

Applying NF membranes with high rejection coefficients of scale forming ions, but relatively low rejection of chloride ion as a pretreatment in seawater desalination opens the possibility for significant increase in R_{NF}. According to the data from Turek et al. [32], it was found that when the TFC-SR2 KOCH NF membrane was selected to soften synthetic seawater solution, higher R_{NF} of 80% was obtained with Ca^{2+}, Mg^{2+}, SO$_4^{2-}$, Cl$^-$, and total hardness rejection of 48.7, 66.9, 90.3, 8.8, and 64.4%, respectively. Comparing TCF-SR2 membrane with mentioned NF1, it can be observed that NF1 membrane has higher rejection coefficient of total hardness.

3.3. CP effect and the real NF separating performance with R_{NF}

3.3.1. CP of the NF modules

CP is a critical factor that can influence the R_{NF}. The variations of CP$_{Mg^{2+}}$, CP$_{SO_4^{2-}}$, and CP$_{Ca^{2+}}$ with R_{NF} are shown in Fig. 7.

It was noted from Fig. 7 that the CP modules of the same divalent ions differed slightly with chemicals dosage changing than NF membrane-type changing. In addition, the CP module of each divalent ion in the seawater NF softening processes differed quite apparently with R_{NF}.

It could be seen that for all the four schemes, as a whole, the increase in the R_{NF} resulted in an increase in CP modules for NF1 module and a sharp increase at the initial stage and then a slight decline of CP modules for NF2 module. According to Eqs. (4)–(5), it
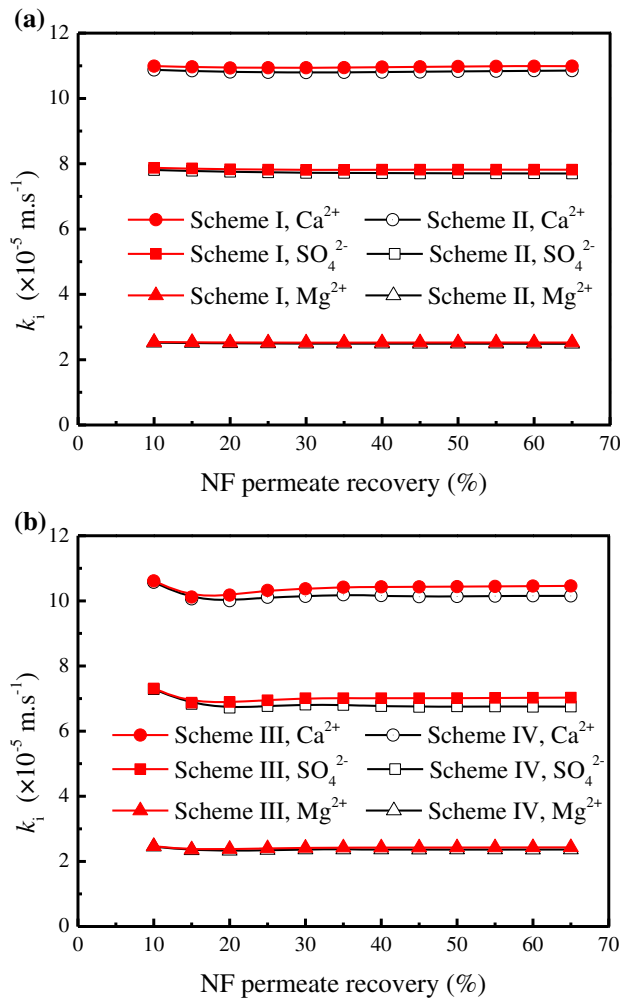
Fig. 8. Mass transfer coefficient k_i of Ca^{2+}, SO$_4^{2-}$, and Mg^{2+} for NF modules with R_{NF} ((a) NF1 and (b) NF2).
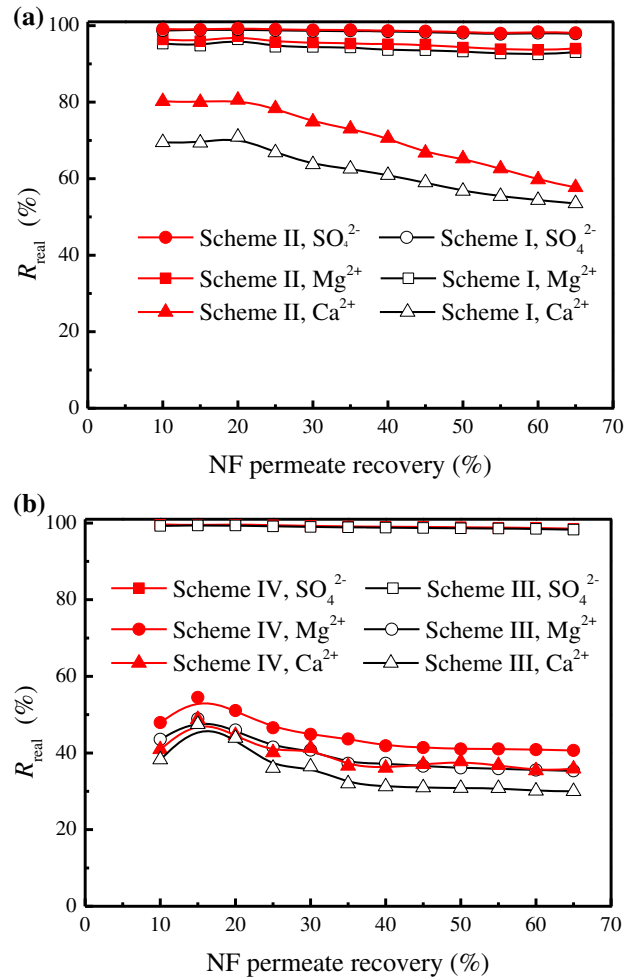
Fig. 9. The variation of the real rejection of SO$_4^{2-}$, Mg^{2+}, and Ca^{2+} ions with R_{NF} ((a) NF1 and (b) NF2).

might be explained by two trade-off effects. On the one hand, the CP module is proportional to solvent flux and the solute concentration in the bulk stream; on the other hand, this value is inversely proportional to the solute mass transfer coefficient and the solute concentration in the permeate stream. These effects control the trend of CP modules with R_{NF}. For example, an ascending of R_{NF} from 10 to 65% resulted in an ascending of $CP_{SO_4^{2-}}$, $CP_{Ca^{2+}}$, and $CP_{Mg^{2+}}$ from 1.018, 1.008 and 1.054 to 1.021, 1.009 and 1.061 in Scheme I process, respectively. The relatively larger $CP_{SO_4^{2-}}$, $CP_{Ca^{2+}}$, and $CP_{Mg^{2+}}$ occurred in Scheme II process are mainly due to the higher values of permeate flux at each fixed R_{NF} (seen in Fig. 4). However, the experimental data (seen in Fig. 7(b)) implies that the former effect, especially solvent flux effect, seems to be dominant to control the variation trend of CP modules for NF2 membrane in Schemes III and IV processes.

It could also be found that under the same R_{NF}, $CP_{Mg^{2+}}$ was much relative higher than $CP_{Ca^{2+}}$. This phenomenon can be well interpreted by the larger difference between the k_i of Mg^{2+} and Ca^{2+}. It can be seen from Eq. (6) that under the same operating conditions and membrane channel geometry, k_i varies with the concentration and diffusivity of ions. On the one hand, there is little difference between the coefficient of diffusion of Mg^{2+} and Ca^{2+}, which are 0.96×10^{-9} and 1.06×10^{-9} m^2 s^{-1}, respectively [33]. On the other hand, the concentration of Mg^{2+} is much higher than that of Ca^{2+} in NF feed solution. Therefore, the k_i of Mg^{2+} is much relative lower than that of Ca^{2+}. The k_i of Mg^{2+}, SO_4^{2-}, and Ca^{2+} calculated according to Eq. (6) are shown in Fig. 8. It could be seen that the k_i values of Ca^{2+} were 4–5 times than those of Mg^{2+} in NF softening processes. Therefore, according to Eqs. (4)–(6), under the same R_{NF}, the $CP_{Mg^{2+}}$ is much relative higher than $CP_{Ca^{2+}}$.

3.3.2. Real rejection of NF membranes

Fig. 9 compares the real rejection of the main scaling-prone ions (Ca^{2+}, Mg^{2+}, and SO_4^{2-}) calculated using CP theory during four schemes at R_{NF} values between 10 and 65%. It can be seen that the SO_4^{2-} rejection of all the four schemes was above 95%. However, for Ca^{2+} and Mg^{2+} ions, the rejection varied greatly from one scheme to another. Higher rejection of Ca^{2+} and Mg^{2+}, a large proportion of which exceed 60% were observed in Schemes I and II processes.

The effect of R_{NF} on the real rejection of total hardness is presented in Fig. 10. It could be seen from Fig. 10 that the real rejection of total hardness in the four schemes decreased with R_{NF} when it was kept above 20%. The real rejection of total hardness by NF1 membrane (in Schemes I and II processes) was relatively stable, and varied only slightly with R_{NF}. A highest real rejection of total hardness was observed in Scheme II process. Table 4 presents the divalent ions composition in feed, retentate streams, and on the membrane surface of NF element with R_{NF} at 60% in Scheme II process. It is worth noting that the Ca^{2+}, Mg^{2+}, and SO_4^{2-} ions concentrations and the total hardness value in NF1 permeate are only around 176, 84, 45, and 798 mg L^{-1}, which are much lower than
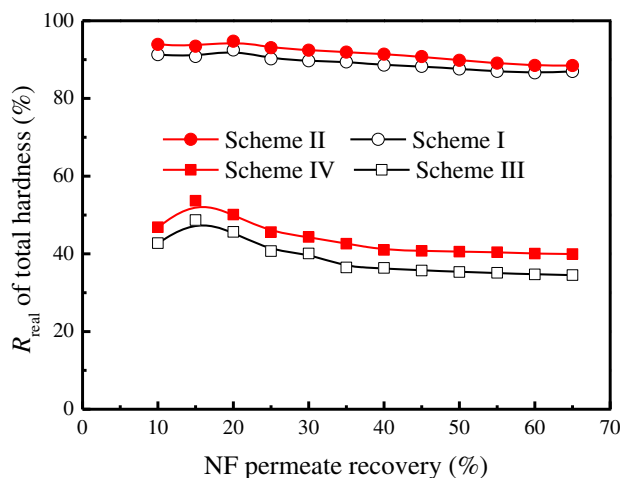
Fig. 10. Trends of the real rejection of total hardness as function of R_{NF}.

Table 4
The composition of NF feed, permeate, and retentate with R_{NF} at 65% in Scheme II

	Conductivity (ms cm^{-1})	Concentration (mg L^{-1})				
		Ca^{2+}	Mg^{2+}	SO$_4^{2-}$	TDS	Total hardness
NF feed	42.6	411	1,296	2,293	34,981	6,564
NF retentate	43.8	426	1,373	2,438	36,011	6,930
NF membrane surface	–	432	1,406	2,505	–	7,089
NF permeate	22.5	176	84	45	17,805	798

that in typical SWRO feed streams, and indicates that NF1 membrane under chemicals dosage yields a relatively high efficiency of seawater softening.

4. Conclusions

The softening performance of NF membranes was evaluated by combing R_{NF} factor and CP effect in treating raw seawater in four different schemes, leading to the outcomes listed below:

(1) The pilot-scale test reveals that under the condition of adding acid and antiscalant, the superior softening performance with 87.7–93.5% of the observed and 88.5–93.9% of the real total hardness removals were achieved by NF1 membrane at constant inlet cross-flow velocity of 0.05 m s^{-1}, operating pressure of 2.02–2.67 MPa, temperature of 21–22℃ and R_r of 1.69–37.16. Under these conditions, a R_{NF}, and permeate flux ranged from 10%, 5.97 L m^{-2} h^{-1} to 65%, 6.93 L m^{-2} h^{-1} were obtained.

(2) The acid and antiscalant dosage induced a significant descent of the R_r under the same R_{NF}, which implied that with chemicals addition, smaller R_r value can be attained for the same higher R_{NF}.

(3) Under the same operating condition, the k_i values of Ca^{2+} ion were 4–5 times than those of Mg^{2+} ion in NF modules, which leads to the relatively higher CP$_{Mg^{2+}}$ than CP$_{Ca^{2+}}$.

(4) The Ca^{2+}, Mg^{2+}, SO$_4^{2-}$ ions concentrations and the total hardness value in NF permeate with R_{NF} at 65% in Scheme II are only around 176, 84, 45, and 798 mg L^{-1}, which are much lower than that in typical SWRO feed streams, and indicates that NF1 membrane under chemicals dosage yields a relatively high efficiency of seawater softening.

Nomenclature

CF	—	concentrate factor, (−)
C_i	—	concentration of species i, (mol m^{-3})
CP	—	concentration polarization module, (−)
d_h	—	hydraulic diameter, (m)
D_i	—	solute diffusion coefficient, (m^2 s^{-1})
k_2	—	the dissociation equilibrium constant of HCO$_3^-$, (−)
k_i	—	mass transfer coefficient, (m s^{-1})
pH	—	the measured retentate water pH, (−)
Q	—	flow rate, (L h^{-1})
R	—	salt rejection, (−)
R_r	—	recycle ratio, (−)
u	—	the cross-flow velocity in the flow channel, (m s^{-1})
R_{NF}	—	NF permeate recovery, (−)
R_{real}	—	real rejection, (−)
R_{obs}	—	observed rejection, (−)
ρ	—	density of the fluid, (kg m^{-3})
v	—	kinematic viscosity, (m^2 s^{-1})

Subscripts

b	—	bulk
i	—	species i
m	—	on membrane surface
p	—	permeate
$r1$	—	retentate stream
$r2$	—	recycle stream

References

[1] W. Fang, L. Shi, R. Wang, Interfacially polymerized composite nanofiltration hollow fiber membranes for low-pressure water softening, J. Membrane Sci. 430 (2013) 129–139.

[2] D. Nanda, K.-L. Tung, C.-C. Hsiung, C.-J. Chuang, R.-C. Ruaan, Y.-C. Chiang, C.-S. Chen, T.-H. Wu, Effect of solution chemistry on water softening using charged nanofiltration membranes, Desalination 234 (2008) 344–353.

[3] L. Setiawan, L. Shi, R. Wang, Dual layer composite nanofiltration hollow fiber membranes for low-pressure water softening, Polymer 55 (2014) 1367–1374.

[4] A.M. Comerton, R.C. Andrews, D.M. Bagley, The influence of natural organic matter and cations on fouled nanofiltration membrane effective molecular weight cut-off, J. Membrane Sci. 327 (2009) 155–163.

[5] R. Rohani, M. Hyland, D. Patterson, A refined one-filtration method for aqueous based nanofiltration and ultrafiltration membrane molecular weight cut-off determination using polyethylene glycols, J. Membrane Sci. 382 (2011) 278–290.

[6] L. Llenas, G. Ribera, X. Martínez-Lladó, M. Rovira, J. de Pablo, Selection of nanofiltration membranes as pretreatment for scaling prevention in SWRO using real seawater, Desalin. Water Treat. 51 (2013) 930–935.

[7] O.A. Hamed, A.M. Hassan, K. Al-Shail, M.A. Farooque, Performance analysis of a trihybrid NF/RO/MSF desalination plant, Desalin. Water Treat. 1 (2009) 215–222.

[8] M. Pontié, J.S. Derauw, S. Plantier, L. Edouard, L. Bailly, Seawater desalination: Nanofiltration-a substitute for reverse osmosis? Desalin. Water Treat. 51 (2013) 485–494.

[9] D.-X. Wang, X.-L. Wang, Y. Tomi, M. Ando, T. Shintani, Modeling the separation performance of nanofiltration membranes for the mixed salts solution, J. Membrane Sci. 280 (2006) 734–743.

[10] A. Figoli, A. Cassano, A. Criscuoli, M.S.I. Mozumder, M.T. Uddin, M.A. Islam, E. Drioli, Influence of operating parameters on the arsenic removal by nanofiltration, Water Res. 44 (2010) 97–104.

[11] Y. Song, J. Xu, Y. Xu, X. Gao, C. Gao, Performance of UF–NF integrated membrane process for seawater softening, Desalination 276 (2011) 109–116.

[12] E. Drioli, A.I. Stankiewicz, F. Macedonio, Membrane engineering in process intensification—An overview, J. Membrane Sci. 380 (2011) 1–8.

[13] B. Su, M. Dou, Y. Wang, X. Gao, C. Gao, Study on seawater nanofiltration softening technology for offshore oilfield polymer solution preparation, Desalin. Water Treat. 51 (2013) 5064–5073.

[14] M.S.H. Bader, Nanofiltration for oil-fields water injection operations: Analysis of osmotic pressure and scale tendency, Desalin. Water Treat. 201 (2006) 114–120.

[15] A.M. Helal, Hybridization—A new trend in desalination, Desalin. Water Treat. 3 (2009) 120–135.

[16] A.M. Hassan, M.A.K. Al-Sofi, A.S. Al-Amoudi, A.T.M. Jamaluddin, A.M. Farooque, A. Rowaili, A.G.I. Dalvi, N.M. Kither, G.M. Mustafa, I.A.R. Al-Tisan, A new approach to membrane and thermal seawater desalination processes using nanofiltration membranes, [Part 1], Desalination 118 (1998) 35–51.

[17] B. Su, T. Wu, Z. Li, X. Cong, X. Gao, C. Gao, Pilot study of seawater nanofiltration softening technology based on integrated membrane system, Desalination 368 (2015) 193–201.

[18] J. Luo, L. Ding, Y. Su, S. Wei, Y. Wan, Concentration polarization in concentrated saline solution during desalination of iron dextran by nanofiltration, J. Membrane Sci. 363 (2010) 170–179.

[19] V. Freger, T.C. Arnot, J.A. Howell, Separation of concentrated organic/inorganic salt mixtures by nanofiltration, J. Membrane Sci. 178 (2000) 185–193.

[20] N. Capelle, P. Moulin, F. Charbit, R. Gallo, Purification of heterocyclic drug derivatives from concentrated saline solution by nanofiltration, J. Membrane Sci. 196 (2002) 125–141.

[21] M.R. Sohrabi, S.S. Madaeni, M. Khosravi, A.M. Ghaedi, Concentration of licorice aqueous solutions using nanofiltration and reverse osmosis membranes, Sep. Purif. Technol. 75 (2010) 121–126.

[22] M. Liu, Z. Lü, Z. Chen, S. Yu, C. Gao, Comparison of reverse osmosis and nanofiltration membranes in the treatment of biologically treated textile effluent for water reuse, Desalination 281 (2011) 372–378.

[23] F. Knops, S. van Hoof, H. Futselaar, L. Broens, Economic evaluation of a new ultrafiltration membrane for pretreatment of seawater reverse osmosis, Desalination 203 (2007) 300–306.

[24] Y. Song, X. Gao, C. Gao, Evaluation of scaling potential in a pilot-scale NF–SWRO integrated seawater desalination system, J. Membrane Sci. 443 (2013) 201–209.

[25] M. Wilf, C. Bartels, Optimization of seawater RO systems design, Desalination 173 (2005) 1–12.

[26] H.-J. Oh, T.-M. Hwang, S. Lee, A simplified simulation model of RO systems for seawater desalination, Desalination 238 (2009) 128–139.

[27] D.-X. Wang, L. Wu, Z.-D. Liao, X.-L. Wang, Y. Tomi, M. Ando, T. Shintani, Modeling the separation performance of nanofiltration membranes for the mixed salts solution with Mg^{2+} and Ca^{2+}, J. Membrane Sci. 284 (2006) 384–392.

[28] L.F. Greenlee, D.F. Lawler, B.D. Freeman, B. Marrot, P. Moulin, Reverse osmosis desalination: Water sources, technology, and today's challenges, Water Res. 43 (2009) 2317–2348.

[29] C.H. Cho, K.Y. Oh, S.K. Kim, J.G. Yeo, P. Sharma, Pervaporative seawater desalination using NaA zeolite membrane: Mechanisms of high water flux and high salt rejection, J. Membrane Sci. 371 (2011) 226–238.

[30] V.V. Nikonenko, A.V. Kovalenko, M.K. Urtenov, N.D. Pismenskaya, J. Han, P. Sistat, G. Pourcelly, Desalination at overlimiting currents: State-of-the-art and perspectives, Desalination 342 (2014) 85–106.

[31] Y. Song, B. Su, X. Gao, C. Gao, Investigation on high NF permeate recovery and scaling potential prediction in NF–SWRO integrated membrane operation, Desalination 330 (2013) 61–69.

[32] M. Turek, M. Chorążewska, Nanofiltration process for seawater desalination—Salt production integrated system, Desalin. Water Treat. 7 (2009) 178–181.

[33] D.X. Wang, M. Su, Z.Y. Yu, Separation performance of a nanofiltration membrane influenced by species and concentration of ions, Desalination 175 (2005) 219–225.